

Characterization of Fe nanorods grown directly from submicron-sized iron grains by thermal evaporation

Chunyu Pan, Zhengjun Zhang,* Xin Su, Ye Zhao, and Jingguo Liu

Department of Materials Science and Engineering, Tsinghua University, Beijing 100084, People's Republic of China

(Received 8 July 2004; published 6 December 2004)

Materials with size down to the nanometer scale exhibit melting points lower than that of their bulk form. This may lead to new catalyst-free approaches for fabricating metal/metal oxides nanostructures. In this Brief Report, we report the observation of Fe nanorods grown directly from submicron-sized Fe grains on Si substrates at $\sim 650^\circ\text{C}$, by thermal evaporation. The iron nanorods are single crystalline, several tens of nanometers in diameter, and several hundred nanometers long, and are coated with a thin (several nanometers thick), single-crystalline Fe_2O_3 layer. The growth of Fe nanorods by this approach is due to the partial melting and iron droplet formation on submicron-sized grains at temperatures much lower than its melting point. This study opens a new way to fabricate metal/metal oxides nanostructures without catalysts, at relatively low substrate temperatures.

DOI: 10.1103/PhysRevB.70.233404

PACS number(s): 61.46.+w

Low-dimensional materials such as nanotubes, nanobelts, and nanowires exhibit outstanding properties that are attractive for modern nanotechnologies, and have thus attracted tremendous efforts in the past years.¹ Among the nanostructures magnetic materials have drawn special attention due to their potential applications in magnetic sensors, ultrahigh-density magnetic storage devices, micromotors, etc.^{2,3} Nevertheless, Fe nanostructures, as a representative of magnetic nanomaterial, can also be employed to catalyze the growth of other materials, e.g., carbon nanotubes and Si nanowires.⁴ Therefore, it is of great importance to make thorough investigations on the synthesis and growth mechanism of iron nanostructures via different means.

There are several approaches available for synthesizing iron nanostructures, for example, sputtering, chemical vapor deposition, electrodeposition, flash evaporation, template-directed growth, and solution-based techniques.⁵⁻¹¹ The Fe nanowires prepared by these approaches could be single-crystalline α -Fe or γ -Fe, or polycrystalline $(\alpha + \gamma)$ -Fe.¹²⁻¹⁴ Here, we report an alternative approach, i.e., growth directly from micro-sized metal grains, to synthesize single-crystalline Fe nanorods. The approach comes from the facts that materials of reduced size have melting points lower than their bulk form^{15,16} and that metal droplets could be formed at temperatures much lower than their melting points depending on the shapes, which is the key of the approach. We found that Fe droplets could be formed at $\sim 650^\circ\text{C}$ in boundaries and sharp edges of micro-sized iron grains, from which the Fe nanorods grow. The advantage of this approach is that it is very simple and that the substrate temperature could be greatly reduced, e.g., the substrate temperature for growing single-crystalline Fe nanorods was $\sim 650^\circ\text{C}$. Since the nanorods were formed directly from the micro-sized metal grains, it might also be applied to fabricate other metal/metal oxide nanostructures.

The substrates used in this study were Si(001). These were cleaned in acetone, alcohol, and deionized water baths supersonically in sequence, and were put inside a spiral coil made with iron wires (99.99% pure) connected to two copper

electrodes in a vacuum chamber. The chamber was pumped to a vacuum on the order of 10^{-3} Torr, and then a voltage (adjusted by a voltage regulator connected to a voltage changer) was applied to the two electrodes, heating up the coil rapidly. The temperature of the coil was measured with a WFH-655 fiber-optical infrared thermometer and that of the silicon substrate was monitored with a K series thermal couple. In our experiment, the coil temperature was monitored to be $\sim 800^\circ\text{C}$ and that of the substrate was measured to be $\sim 650^\circ\text{C}$, and the typical deposition time was 2 min. The morphology and structure of iron deposits on the silicon substrates were examined and characterized by scanning (SEM) and transmission electron microscopes (TEM), and high-resolution TEM (HRTEM), selected area diffraction (SAD), energy dispersive x-ray spectrometer (EDX), and Raman spectroscopy.

Figures 1(a) and 1(b) show representative SEM micrographs of Fe nanorods deposited on silicon substrates at $\sim 650^\circ\text{C}$ within a deposition time of 2 min. The images were taken with a JSM-6301F field emission SEM working at 20 kV. One sees that besides the submicron-sized iron grains, there are number of iron nanorods (several hundred nanometers long and several tens of nanometers in diameter) randomly grown from the submicron-sized iron grains. Figure 1(b) shows the random orientation and diameter of iron nanorods deposited. Figures 1(c) and 1(d) show typical TEM micrographs of the iron nanorods prepared by this approach. The images were taken with a JEOL 200 CX TEM, working at 200 kV. It is seen that for typical nanorods, their diameter is several tens of nanometers, and that the iron nanorods were totally sheathed by a thin (several nanometers thick) α - Fe_2O_3 layer, which was probably formed during the deposition process due to the existence of oxygen in the low vacuum. Figures 1(e) and 1(f) show a typical HRTEM image and the corresponding SAD pattern of the iron nanorods. The HRTEM image and the SAD pattern were taken with a JEM-2010F field emission TEM working at 200 kV. One sees that the nanorod contains a thick Fe core and a thin (~ 3 nm thick) α - Fe_2O_3 layer, and that the Fe core and α - Fe_2O_3 thin

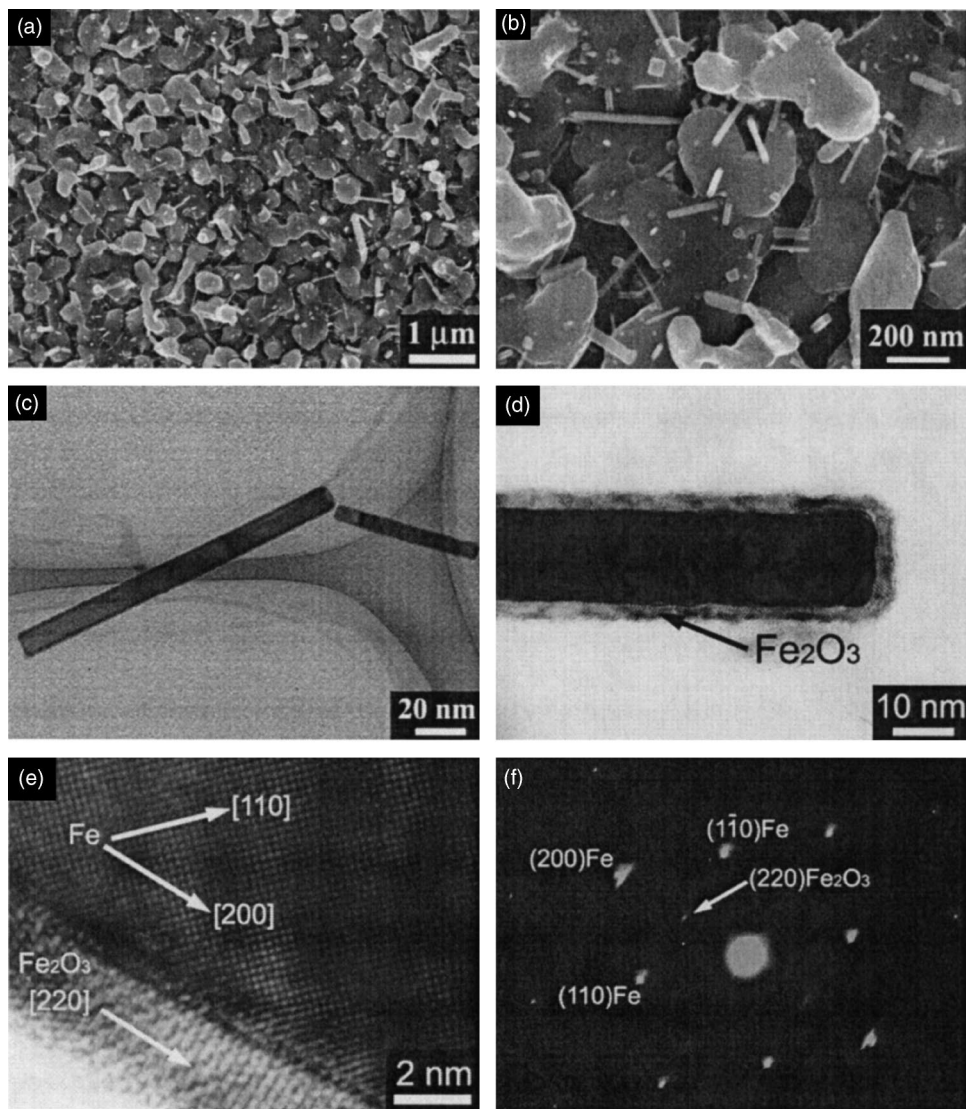


FIG. 1. (a) Low-magnification and (b) high-magnification SEM micrographs of Fe nanorods deposited on Si substrates at $\sim 650^\circ\text{C}$; (c) and (d) are typical TEM images showing the length, diameter, and structure of the Fe nanorods; (e) and (f) are the HRTEM image and the corresponding SAD pattern of a Fe nanorod, showing that the Fe core and the Fe_2O_3 sheath are both single crystalline.

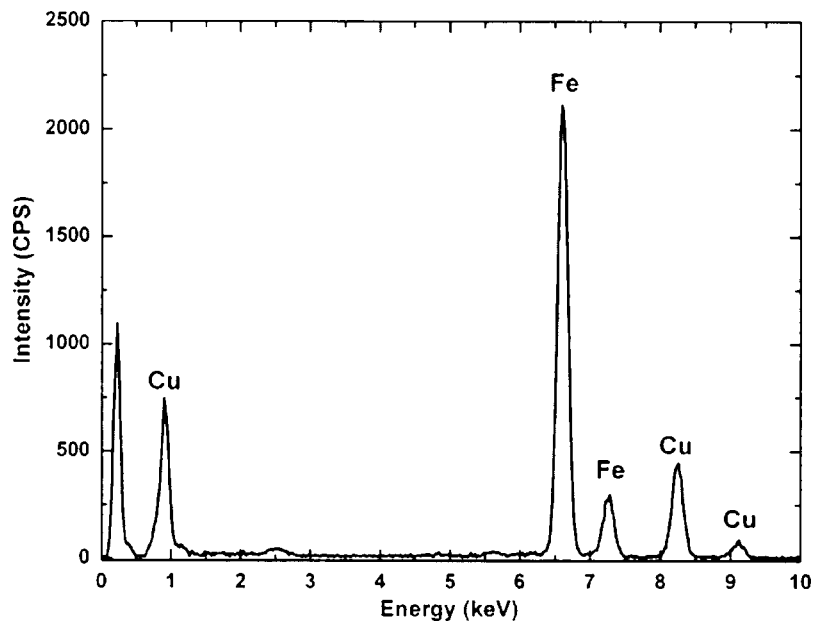


FIG. 2. A typical EDX spectrum of Fe nanorods, showing that the nanorods contain mainly Fe.

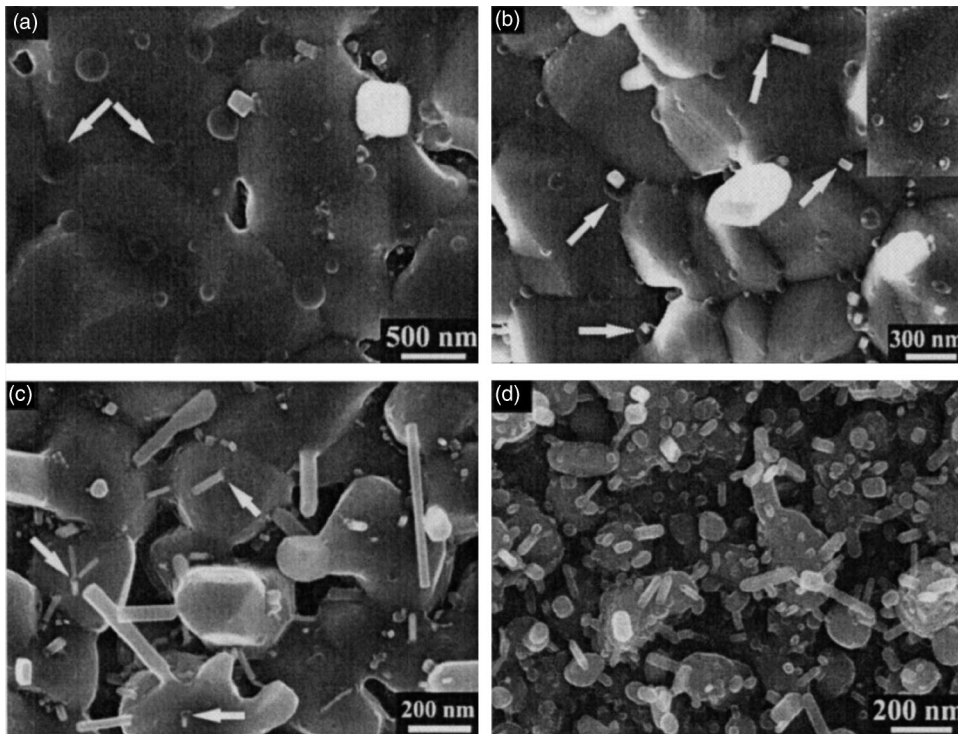


FIG. 3. SEM micrographs of the deposits grown on the silicon substrates at various stages. (a) At the beginning submicron-sized iron grains deposited and iron droplets (see arrows) formed at boundaries and sharp edges of the grains. (b) Fe nanorods nucleated from the droplets (see arrows). Inset shows the nucleation of Fe nanorods from small droplets at the sharp edges of the grains. (c) Fe nanorods grew longer (see arrows). (d) Developed Fe nanorods covering the submicron-sized iron grains at prolonged deposition.

layer are all single crystalline. From the HRTEM image, we did not observe any axial screw dislocations, which are known as the key features of whisker growth.

The existence of Fe in the nanorods was identified with EDX analysis. Figure 2 shows a typical EDX spectrum of an individual nanorod obtained with a JEM-2010F field emission TEM working at 200 kV. The spectrum shows clearly that the nanorods contain mainly Fe. The Cu signals are from the copper grid. The absence of oxygen signals in the spectrum is probably due to its limited amount in the nanorod. Considering the HRTEM, SAD, and EDX analysis, we thus concluded that the nanorods produced by this approach are single-crystalline Fe nanorods sheathed by a thin, single-crystalline α -Fe₂O₃ layer that was formed due to the oxidation of Fe in the low vacuum.

The present approach is actually a simple thermal evaporation process. We know that the heated iron coil could release iron atoms that deposit on the silicon substrate and form iron particles [as shown in Figs. 1(a) and 1(b), they formed submicron-sized grains]. The growth of Fe nanorods by this approach is therefore very intriguing since it might provide a new way to prepare metal nanorods at relatively low substrate temperatures. To make clear the growth mechanism of the Fe nanorods, we stopped the deposition at various stages to observe the morphology of the deposits. Figure 3 shows typical SEM images of the deposits obtained at increased deposition time. We note that at the beginning of deposition [see Fig. 3(a)], Fe atoms evaporated from the iron coil ($\sim 800^\circ\text{C}$) deposited on the silicon substrate ($\sim 650^\circ\text{C}$) and formed submicron-sized grains of irregular shapes. Interestingly, at boundaries and sharp edges of iron

grains, droplets [see arrows indicated in Fig. 3(a)] were formed at a temperature as low as $\sim 650^\circ\text{C}$, which is much lower than the melting temperature of pure iron ($\sim 1536^\circ\text{C}$). These droplets acted as nucleation sites of Fe nanorods. As indicated by the arrows in Fig. 3(b), Fe nanorods (several tens of nanometers in diameter and of a rectangular shape) started to grow from these droplets. At prolonged deposition, the nucleated Fe nanorods became longer [see arrows in Fig. 3(c)], and more Fe nanorods started to grow from the droplets [see Fig. 3(d)], finally forming a number of Fe nanorods from the submicron-sized iron grains. Therefore, once we find ways to control the alignment of the Fe nanorods by the current approach, this growth phenomenon might be applicable to fabricate aligned Fe nanorods on flat substrates, for applications as data (magnetic) storage media, or templates to prepare other nanomaterials, etc.

In summary, we observed the melting and droplet formation of Fe on submicron-sized iron grains at a temperature of $\sim 650^\circ\text{C}$, which is much lower than its melting point, and the growth of single-crystalline Fe nanorods directly from droplets at the melted areas of the submicron-sized grains. This study illuminates a possible catalyst-free way to prepare metal/metal oxides nanostructures at relatively low substrate temperatures.

The authors are grateful to the financial support by the National Natural Science Foundation of China (50225102, 50131020), by FANEDD of the Education Ministry of China (200133), and the administration of Tsinghua University.

*Corresponding author. Electronic address: zjzhang@tsinghua.edu.cn

- ¹See, for example, S. Iijima, *Nature (London)* **354**, 56 (1991); G. R. Patake, F. Krumeich, and R. Nesper, *Angew. Chem., Int. Ed.* **41**, 2446 (2002).
- ²G. A. Prinz, *Science* **282**, 1660 (1998).
- ³S. Y. Chou, M. S. Wei, P. R. Krauss, and P. B. Fisher, *J. Appl. Phys.* **76**, 6673 (1994).
- ⁴Y. H. Yang *et al.*, *J. Phys. Chem. B* **108**, 846 (2003).
- ⁵C. G. Granqvist, *Handbook of Inorganic Electrochromic Materials* (Elsevier, Amsterdam, 1995), reprinted 2002.
- ⁶O. R. Lourie, *Chem. Mater.* **12**, 1808 (2000).
- ⁷M. Z. Zhang *et al.*, *Adv. Mater. (Weinheim, Ger.)* **16**, 409 (2004).
- ⁸C. Julien, A. Khelifa, O. M. Hussain, and G. A. Nazri, *J. Cryst. Growth* **156**, 235 (1995).
- ⁹C. Julien, B. Yebka, and G. A. Nazri, *Mater. Sci. Eng., B* **38**, 65 (1996).
- ¹⁰S. J. Park *et al.*, *J. Am. Chem. Soc.* **122**, 8581 (2000).
- ¹¹L. Manna and E. C. Scher, *J. Am. Chem. Soc.* **122**, 12700 (2000).
- ¹²C. Prados *et al.*, *IEEE Trans. Magn.* **37**, 2117 (2001).
- ¹³H. J. Elmers *et al.*, *Phys. Rev. Lett.* **73**, 898 (1994).
- ¹⁴P. M. Paulus, F. Luis, M. Kröll, G. Schmid, and L. J. de Jongh, *J. Magn. Magn. Mater.* **224**, 180 (2001).
- ¹⁵S. L. Lai, J. Y. Guo, V. Petrova, G. Ramanath, and L. H. Allen, *Phys. Rev. Lett.* **77**, 99 (1996).
- ¹⁶C. E. Bottani *et al.*, *Phys. Rev. B* **59**, R15 601 (1999).